Exploring the Role of Different Drug Transport Routes in Permeability Screening

Pär Matsson,[†] Christel A. S. Bergström,[†] Naoki Nagahara,[†] Staffan Tavelin,[†] Ulf Norinder,[†,‡] and Per Artursson*,[†]

Center of Pharmaceutical Informatics, Department of Pharmacy, Uppsala University, Uppsala Biomedical Center, P.O. Box 580, SE-751 23 Uppsala, Sweden, and Department of Medicinal Chemistry, AstraZeneca Research and Development, SE-151 85 Södertälje, Sweden

Received April 15, 2004

The influence of different drug transport routes in intestinal drug permeability screening assays was studied. Three experimental models were compared: the small-intestine-like 2/4/A1 cell model, which has a leaky paracellular pathway, the Caco-2 cell model, which has a tighter paracellular pathway, and artificial hexadecane membranes (HDMs), which exclusively model the passive transcellular pathway. The models were investigated regarding their ability to divide passively and actively transported compounds into two permeability classes and to rank compounds according to human intestinal absorption. In silico permeability models based on two-dimensional (2D) and three-dimensional (3D) molecular descriptors were also developed and validated using external test sets. The cell-based models classified 80% of the acceptably absorbed compounds (FA ≥ 30%) correctly, compared to 60% correct classifications using the HDM model. The best compound ranking was obtained with 2/4/A1 ($r_s = 0.74$; $r_s = 0.95$ after removing actively transported outliers). The in silico model based on 2/4/A1 permeability gave results of similar quality to those obtained when using experimental permeability, and it was also better than the experimental HDM model at compound ranking ($r_s = 0.85$ and 0.47, respectively). We conclude that the paracellular transport pathway present in the cell models plays a significant role in models used for intestinal permeability screening and that 2/4/A1 in vitro and in silico models are promising alternatives for drug discovery permeability screening.

Introduction

Intestinal drug permeability is considered to be one of the two major barriers to intestinal drug absorption, solubility being the other.[1] For the assessment of intestinal drug permeability, epithelial cell culture models such as Caco-2 are routinely used.[2−6] One of the reasons for the widespread use of Caco-2 assays is the versatility of the cell line, which allows studies not only of passive diffusion processes but also, after modifications, of the experimental setup of active drug transport and efflux systems and presystemic drug metabolism.[7,8] However, this versatility is considered to be a potential weakness of the Caco-2 cell culture model in the screening setting. For instance, the Caco-2 cell line forms very tight monolayers compared to the human small intestine, which has been explained by the colonic origin of the cell line.[9] Also, in some combinatorial libraries, an unexpectedly large percentage of the compounds is found to be substrates for efflux proteins in Caco-2 cells, whereas the in vivo relevance of these findings remains unclear.[10]

A preferred solution to these issues is the adoption of a reductionist approach, by which different mechanisms affecting intestinal drug absorption are studied in separate experimental systems. Different alternative models, such as the intestinal epithelial cell line 2/4/A1[11] and the filter-immobilized hexadecane membrane (HDM) model,[12] have been used to study the dominating passive transport pathways in the absence of active transport, while, for active transport, studies in expression systems that overexpress a specific active drug transporter are generally favored.[13,14]

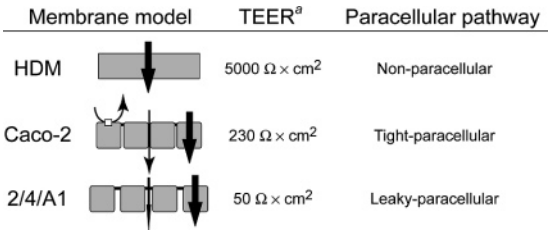

Figure 1. Schematic illustration of the membrane models used in this study. [a]TEER: transepithelial electrical resistance is a measure of the resistance to ion flux across the membrane. Because the paracellular pathway greatly affects TEER, a high value will reflect a tighter membrane. In addition to passive permeability, active efflux transporters can influence permeability values in the Caco-2 model under the applied experimental conditions.

The 2/4/A1 cells lack functional expression of several important active drug transporters and form monolayers with a more leaky, small-intestine-like paracellular pathway than that of Caco-2 monolayers (Figure 1). As a result, the 2/4/A1 cell line is thought to better mimic the epithelial barrier to passive drug transport in vivo.[15] Different artificial membrane models, such as HDM- and phospholipid-based parallel artificial membrane permeation assays (PAMPA), completely lack active transport pathways, and, in addition, the paracellular pathway is absent in these models (Figure 1).[12,16−20] Thus, the popularity of the artificial membrane models

* Author to whom correspondence should be addressed. Telephone: +46 18 471 44 71. Fax: +46 18 471 44 84. E-mail: Per.Artursson@farmaci.uu.se.
[†] Uppsala University.
[‡] AstraZeneca Research and Development.

10.1021/jm049711o CCC: $30.25
Published on Web 12/18/2004

relies on the assumption that the transcellular barrier is the dominant barrier to drug absorption. This assumption is supported by numerous studies indicating that intestinal drug absorption of soluble drugs is correlated to passive drug permeability.[12,15,18,21−23] Passive membrane permeability is strongly related to relatively simple molecular descriptors, which has made it possible to develop in silico models that predict the permeability of passively transported drugs. Examples include rule-based models such as Lipinski's rule of five[1] and correlations with hydrogen bond descriptors[24,25] or molecular surface area descriptors such as the polar surface area (PSA).[22,26−31] Thus, in principle it is possible to develop in silico models that predict drug permeability from molecular descriptors, but whether such models can compete with experimental permeability models in a screening setting is not yet clear.[32]

A potential bias seen in studies of in vitro and in silico models intended to predict drug absorption is that the data sets are generally enriched in completely absorbed compounds (Figure 2).[12,18,23,25,33−39] This is probably because the data sets are based on orally administered marketed drugs that have been selected partly on the basis of their favorable absorption properties. Models based on such skewed data sets are often able to distinguish fairly well between completely (≥80%) and poorly absorbed compounds and can rapidly give useful indications of the expected average permeability of compound libraries early in the drug discovery process. However, compounds with moderate absorption properties may also be of interest in the early phases of drug discovery, and in our opinion it would be advantageous to include such compounds in the evaluation of permeability models. The need to include a significant number of incompletely absorbed compounds in the data set is further emphasized during lead optimization, when it is desirable to rank compounds according to their absorption properties.

Another potential bias arises because the data sets are generally based on passively transported compounds and no consideration is given to the potential influence of active transport.[22,40] Although this approach gives better models of passive permeability, the models generate selective information only about the passive route, and their performance in the screening of data sets that include actively transported compounds remains to be investigated.

In this work, we compare the widely used permeability model Caco-2 with two emerging alternative models regarding ability to predict the fraction absorbed after oral drug administration in humans (FA). To avoid problems arising from the large interlaboratory variation observed for permeability data, only data determined in our own laboratory under standardized experimental conditions were used. For instance, unstirred water layer effects in the permeability determinations were minimized by using high stirring rates, as described by Stenberg et al.[22] The data set was carefully selected to evenly cover the entire range of FA in humans (0−100%, Figure 2h) and to be widely spread in the molecular descriptor space. In addition, we included a number of drugs that are at least partly actively transported, to better reflect the discovery situation where transporter affinities are unknown and

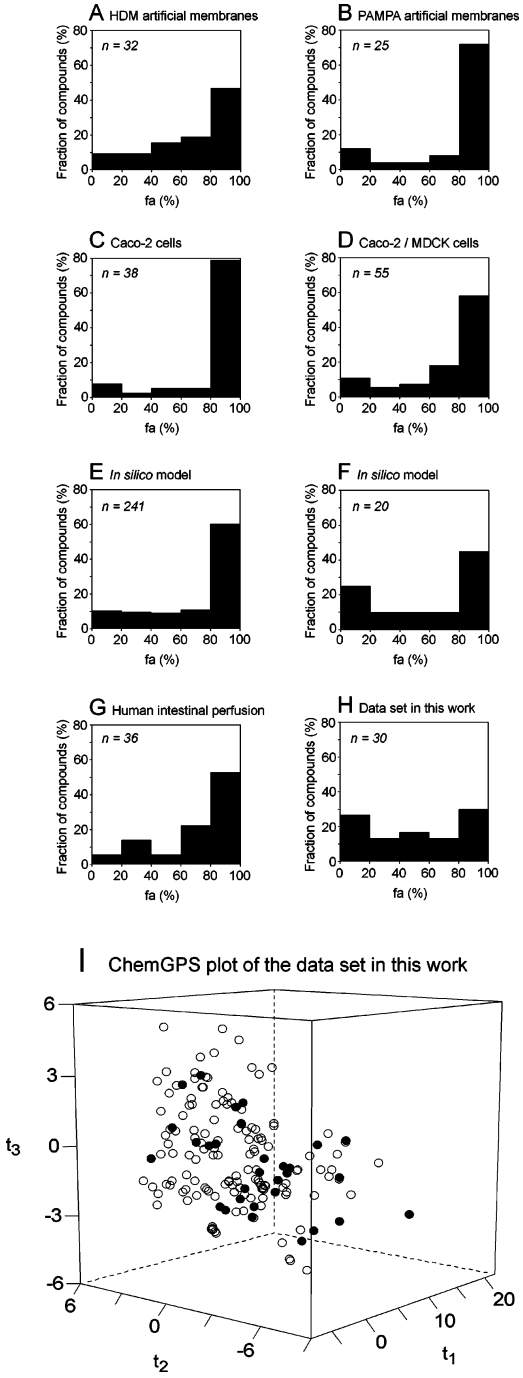

Figure 2. Distribution of data sets used for prediction of FA: (A) ref 12, (B) ref 18, (C) ref 23, (D) ref 39, (E) ref 25, (F) ref 27, (G) refs 33−38 and 58, (H) this study; (I) ChemGPS plot of the data set in this study and of a reference set of orally administered drugs. The closed symbols represent the data set used in this study, and the open symbols represent 150 registered orally administered drugs taken from the Physician's Desk Reference.

to further stress mechanistic differences between the experimental models (Table 1). Caco-2 cells express various active transporters that are not present in the 2/4/A1 and HDM models, including the efflux transporter P-glycoprotein (P-gp).[41,42] Finally, the experimental results were used to develop in silico models of intestinal permeability. The experimental and in silico models were evaluated both for their ability to classify compounds as poorly or acceptably absorbed and for their ability to rank compounds according to FA. In

Table 1. Permeability Coefficients and Intestinal Absorption of the Compounds in the Data Set

drug[a]	active transport mechanism	additional passive (paracellular) route	P_{app} a−b (cm/s × 10^6)			mass balance (%) HDM	FA (%)[v]
			Caco-2	2/4/A1	HDM		
1 alfentanil			270 ± 13°	440 ± 14[o]	770 ± 14°	95[g]	100
2 glycylsarcosine*	PEPT1[b]	+	0.50 ± 0.07[p]	11 ± 1.9[p]	0.25 ± 0.090	92	100
3 metoprolol			91 ± 4.0[q]	190 ± 8.3[u]	8.6 ± 1.1	86	100
4 propranolol			204 ± 17[g]	240 ± 44[u]	58 ± 7.7	49	100
5 antipyrine			215 ± 11[e]	250 ± 10.7[u]	11 ± 1.5	107	97
6 alprenolol*			240 ± 14[q]	290 ± 12[u]	160 ± 10	110	96
7 pindolol		+	55 ± 0.60[r]	67 ± 7.1[u]	0.73 ± 0.072	100	92
8 digoxin*	P-gp[c]		1.3 ± 0.14[n]	6.7 ± 1.1[n]	0.12 ± 0.018	96	81
9 cimetidine*	P-gp; OCT1[d]	+	0.67 ± 0.060°	39 ± 1.9°	0.085 ± 0.014°	93[g]	80
10 terbutaline		+	0.23 ± 0.03[g]	41 ± 0.72[u]	0.96 ± 0.37	96	73
11 creatinine		+	1.2 ± 0.068[s]	21 ± 1.7[s]	0.12 ± 0.037	89	70
12 metolazone	P-gp[e]		4.3 ± 0.39[e]	14 ± 0.54[s]	1.1 ± 0.12	104	64
13 methotrexate*	RFC[f]		0.030 ± 0.009[t]	5.2 ± 0.8[g]	0.020 ± 0.004	92	59
14 metformin*		+	0.66 ± 0.16[s]	20 ± 4.1[s]	0.51 ± 0.30	115	55
15 atenolol*		+	1.0 ± 0.13[q]	19 ± 2.3[s]	0.56 ± 0.081	103	54
16 lobucavir	ENT2[g]		0.88 ± 0.13[s]	14 ± 2.1[s]	0.057 ± 0.003	92	50
17 didanosine		+	0.25 ± 0.10[s]	14 ± 0.70[s]	0.099 ± 0.010	84	42
18 valaciclovir	PEPT1[h]		2.3 ± 0.18[g]	35 ± 13.6[g]	0.39 ± 0.15	91	36
19 nadolol	P-gp[i]	+	0.28 ± 0.038[s]	14 ± 2.7[s]	0.032 ± 0.031	69	30
20 sulpiride*	P-gp[e]		0.21 ± 0.012[e]	11 ± 1.4[s]	0.43 ± 0.18	102	30
21 mannitol		+	0.19± 0.014[e]	11 ± 1.2[s]	0.017 ± 0.008	95	26
22 aciclovir	ENT2[j]	+	0.38 ± 0.005[s]	8.2 ± 0.82[s]	0.034 ± 0.013	93	19
23 foscarnet	NAP1[k]	+	0.043 ± 0.004[e]	9.5 ± 0.32[s]	0.36 ± 0.30	91	17
24 sulfasalazine	MRP2; OAT[l]		0.16 ± 0.021[e]	9.6 ± 0.86[s]	0.028 ± 0.011	96	12
25 ganciclovir*	ENT2[m]		0.23 ± 0.067[s]	8.7 ± 1.4[s]	6.7 ± 2.7	97	5
26 clodronic acid		+	0.059 ± 0.036[s]	4.5 ± 0.40[s]	12 ± 1.1	95	3
27 olsalazine		+	0.050 ± 0.007[g]	5.5 ± 0.10[u]	0.066 ± 0.032	102	3
28 lactulose		+	0.27 ± 0.064[e]	8.9 ± 3.6[s]	0.081 ± 0.017	98	1
29 raffinose*		+	0.047 ± 0.004[e]	5.9 ± 0.32[s]	0.051 ± 0.013	92	0
30 mitoxantrone	P-gp; ABCG2[n]		2.3 ± 0.16[n]	7.3 ± 1.1[n]	0.74 ± 0.060	48	n.a.[w]
mean CV (%)			14	12	33		

[a] Substances marked with an asterisk (*) are included in the test set. All compounds are assumed to exhibit passive transcellular diffusion to some extent. + = passive paracellular diffusion; ABCG2 = substrate for the ABCG2 (BCRP) transporter; ENT2 = substrate for the purine nucleobase carrier (SLC29A2, not active in Caco-2); MRP2 = substrate for the multidrug-resistance-associated protein 2 (ABCC2); NAP1 = substrate for the sodium/phosphate cotransporter (SLC20); OAT = substrate for an organic anion transporter (SLCO/SLC22); OCT1 = substrate for the organic cation transporter 1 (SLC22A1); PEPT1 = substrate for the H^+-dependent oligopeptide transporter (SLC15A1, not active in Caco-2 in the absence of a pH gradient); P-gp = substrate for P-glycoprotein (ABCB1); RFC = substrate for the human reduced folate carrier (SLC19A1, not active in Caco-2). [b] Reference 43. [c] Reference 44. [d] Reference 45. [e] Reference 22. [f] Reference 61. [g] Unpublished results. [h] Reference 46. [i] Reference 47. [j] Reference 48. [k] Reference 51. [l] Reference 50. [m] Reference 49. [n] Reference 13. [o] Reference 53. [p] Reference 11. [q] Reference 30. [r] Reference 26. [s] Reference 15. [t] Reference 29. [u] Reference 52. [v] References 15, 22, 25, and 26. [w] Human intestinal absorption data not available. Permeability data for mitoxantrone was used in generating in silico permeability models.

addition, the predictive power of the in silico models was evaluated using a set of well-characterized drug compounds for external validation.

Results and Discussion

Data Set Distribution. A ChemGPS analysis[54] (Figure 2i) showed that the data set in this work was evenly spread in the structural space of orally administered drugs. In addition, a principal component analysis (PCA) based on two-dimensional (2D) and three-dimensional (3D) descriptors of the studied compounds did not show any apparent clustering of compounds, indicating that the data set was structurally diverse (Supporting Information). The diversity was further corroborated by a large spread in calculated properties such as molecular weight, polar surface area (PSA), and octanol−water partition coefficient (ClogP) (Supporting Information, Table 1).

Correlation between Permeability and Intestinal Absorption. Sigmoidal relationships between FA and P_{app} were observed in all three models, which is in agreement with previous observations (Figure 3).[12,15,16,21,22] A nonlinear curve fit showed that the training set P_{app} data from each experimental model could be adequately described by an empirical sigmoidal function and that the fit to the sigmoidal relationship was stronger for 2/4/A1 ($r^2 = 0.87$) than for Caco-2 ($r^2 = 0.72$) and HDM ($r^2 = 0.58$; $r^2 = 0.71$ when excluding outliers ganciclovir and clodronic acid).

In general, P_{app} in the HDM and Caco-2 models was comparable, especially for the high-permeability compounds (Supporting Information, Figure 3 and Table 2). However, P_{app} in the small-intestine-like 2/4/A1 cell culture model was up to 2 log units higher than that in the other experimental models (Figure 3d); i.e., it was quantitatively comparable to those observed in the human jejunum.[36] We conclude that this difference is caused by a larger influence of the paracellular pathway in the 2/4/A1 cell monolayers.[15] The more narrow range of P_{app} in the 2/4/A1 model is also in agreement with human in vivo perfusion data.[15,36]

Permeability Classification Models. In the early stages of the drug discovery process, it is often considered to be sufficient to classify compounds in a binary fashion, i.e., as acceptably or poorly absorbed. The sigmoidal relationships in Figure 3 were therefore used to determine limiting P_{app} values that divided the compounds into two classes: poorly or acceptably absorbed. A rather high cutoff value of FA ≥ 90% is often

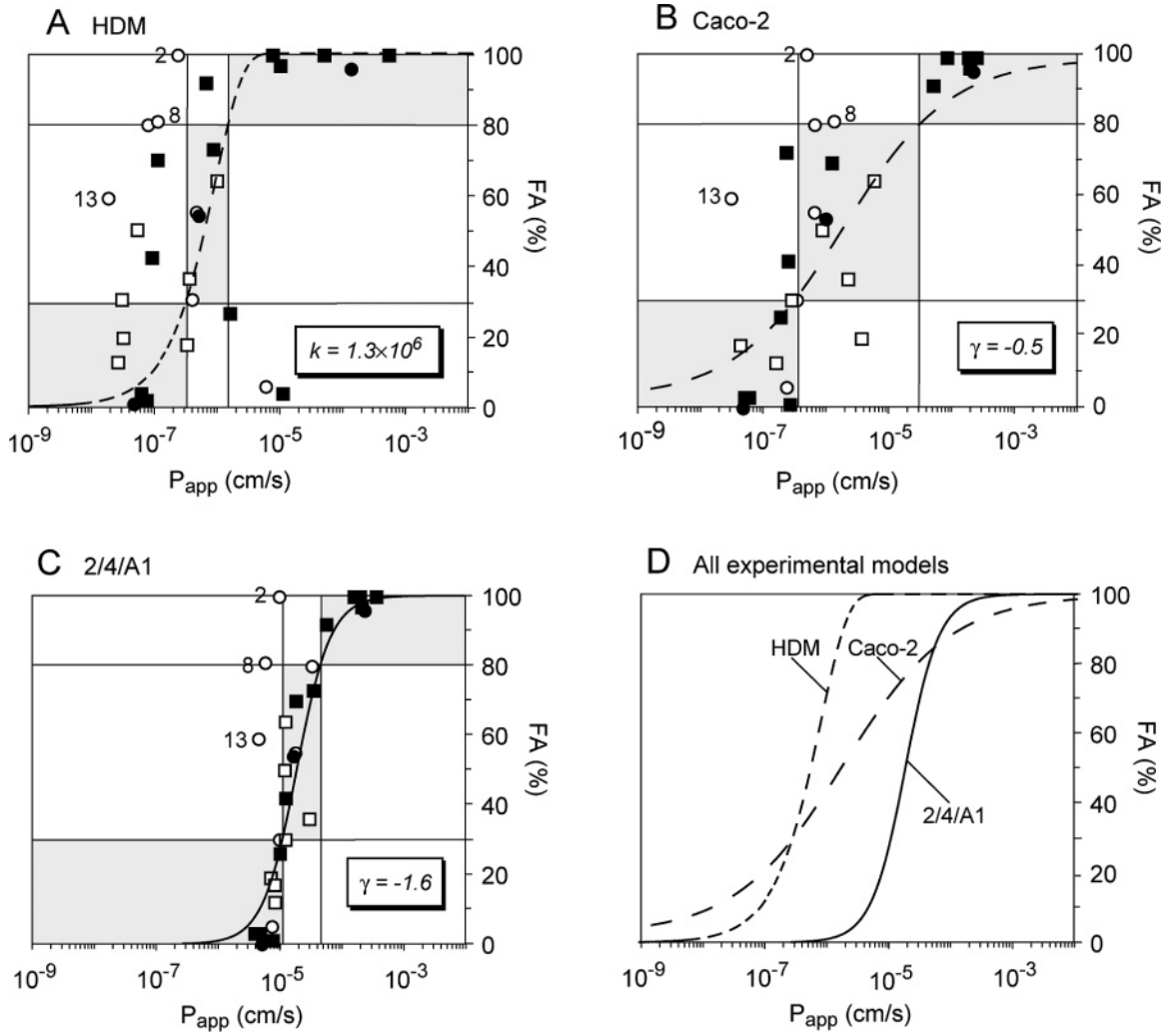

Figure 3. Relationships between FA and permeability coefficients determined in (A) HDM, (B) Caco-2, (C) 2/4/A1, and (D) all models. Squares denote compounds in the training set and circles compounds in the test set. Closed symbols, passively transported compounds; open symbols, actively transported compounds. Short dashed line, sigmoidal curve fit for HDM; long dashed line, Caco-2; solid line, 2/4/A1. The regression coefficient for each sigmoidal curve fit is presented in the corresponding graph.

Table 2. Percentage of Compounds that Were Correctly Classified Using Experimental P_{app} Data

		correctly classified as	
FA class limit[a]	membrane model	acceptably absorbed[b]	poorly absorbed[e]
80%	HDM	56%[c]	85%[d]
	Caco-2	67%[c]	100%[d]
	2/4/A1	67%[c]	100%[d]
30%	HDM	60%[d]	56%[c]
	Caco-2	80%[d]	89%[c]
	2/4/A1	80%[d]	100%[c]

[a] Limiting value of FA used to divide compounds into two absorption classes. [b] Fraction of the compounds correctly classified as *above* the FA limit. [c] $n = 9$. [d] $n = 20$. [e] Fraction of the compounds correctly classified as *below* the FA limit.

chosen for such classification, as recommended in the biological classification system (BCS) implemented by the Food and Drug Administration (FDA).[56,57] When high FA cutoff values (80−90%) were used in this study, the three experimental models classified the data set equally well. However, a large fraction (∼30−40%) of the compounds was falsely predicted as being poorly absorbed (Table 2). This relatively high figure was probably a result of our more evenly distributed data set (Figure 2h). Models based on data sets that are biased toward completely absorbed compounds tend to predict high permeability compounds well but lack precision when predicting poorly permeable compounds.[18,32] In contrast, our data set is evenly distributed regarding FA, and it could therefore be expected that a larger fraction of the highly permeable compounds would be underestimated.

The BCS implemented by FDA has been developed for drug development purposes and reflects a desire to identify well-absorbed compounds that can be subjected to a waiver in bioequivalence studies. In contrast, for permeability screening early on in the drug discovery process, it is often relevant to also identify compounds with an FA significantly lower than 80%. Consultations with colleagues in several pharmaceutical companies indicated that in many drug discovery programs an FA of around 30% is considered as an acceptable starting point. In line with these commonly used values, we selected an FA cutoff of 30% for the purpose of this study.

The cell-based experimental models were comparable at classifying the data set compounds as acceptably (FA ≥ 30%) or poorly (FA < 30%) absorbed (Table 2). 80% of the acceptably absorbed compounds were correctly classified by the two cell-based models. The discriminating power of the HDM model was lower, with 60% of

the acceptably absorbed compounds being correctly classified. We propose that this was mainly because our data set included poorly absorbed compounds with a lower transmembrane permeability, which utilized the alternative paracellular route in the cell culture models, i.e., a transport route that is not available in the artificial HDM membranes.

Ranking of Compounds. In later stages of the drug discovery process, i.e., during lead optimization, it is of interest to rank compounds with regard to FA. It could be argued that a ranking according to human intestinal P_{eff} data would be more relevant, but unfortunately this was not possible, because the available P_{eff} database is strongly biased toward completely absorbed compounds (Figure 2g).[33−38,58]

The rank order correlation between FA and experimentally determined P_{app} was considerably stronger for 2/4/A1 (r_s = 0.74) and Caco-2 (r_s = 0.73) compared to HDM (r_s = 0.47, Figure 4, Table 3). To exclude the possibility that the low rank order correlation between FA and HDM P_{app} was related to the larger average CV obtained in the HDM experiments (Table 1), a variable scrambling procedure was used in which a normally distributed error was added to the Caco-2 and 2/4/A1 P_{app} values. This procedure did not result in any significant deterioration of the relationship between Caco-2 and 2/4/A1 P_{app} and FA, which indicates that the differences in rank order correlations between the membrane models are due to inherent differences between the models (Supporting Information).

Attempts have been made to theoretically include the paracellular pathway in artificial membrane permeability data by calculating the paracellular permeability from size and charge restrictions to drug transport through the paracellular pores.[59,60] Use of this approach for the compounds in this study resulted in lower scatter in the sigmoidal relationship between calculated total P_{app} and FA than when using the original transcellular HDM P_{app} data. The scatter in the HDM rank order correlation was also reduced, but remaining outliers resulted in that the rank order correlation coefficient did not improve significantly (r_s = 0.48 when the paracellular pathway was included). We conclude that by accounting for a paracellular route in artificial membranes it is possible to improve the correlation to FA to some extent but not to the level of the 2/4/A1 correlation.

Notably, only three significant outliers (digoxin, glycylsarcosine, and methotrexate) were seen in the data from the 2/4/A1 model. Two of the outliers can be explained by active uptake mechanisms not present in the 2/4/A1 cells. In vivo, glycylsarcosine is a substrate for the PepT1 di/tripeptide uptake transporter,[43] and methotrexate is a substrate for the reduced folate carrier,[61] none of which are functionally expressed in the 2/4/A1 cell line.[11] The absence of these active pathways can explain why the 2/4/A1 model underestimated the FA for these two compounds. The underestimation of the P-gp substrate digoxin by the 2/4/A1 model could be related to the fact that compounds with a relatively low permeability coefficient may have time to encounter a larger absorptive surface area in the intestine.[3] This would compensate for the low permeability and result in an almost complete absorption in vivo. When the three outliers were removed, the 2/4/A1 rank order correlation became excellent (r_s = 0.95).

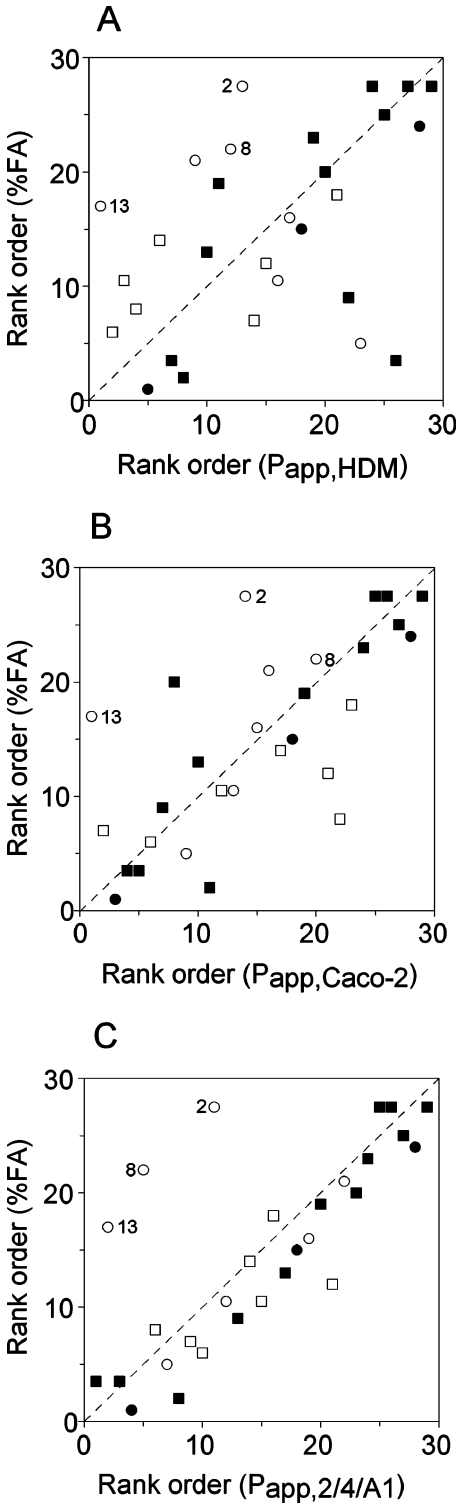

Figure 4. Spearman rank order correlation between FA and experimental P_{app} determined in HDM, Caco-2, and 2/4/A1. Squares denote compounds in the training set and circles compounds in the test set. Closed symbols, passively transported compounds; open symbols, actively transported compounds.

Interestingly, all of the other compounds in the data set lay within the linear rank order relationship, despite the fact that several of them are at least partly transported by various active transporters (Table 1). The relevance of active transport in the human intestine

Table 3. Spearman Rank Order Correlation between FA and P_{app}

	Spearman rank order correlation coefficient	
membrane model	all compounds	outliers[a] removed
HDM	0.47	0.57[b]
Caco-2	0.73	0.82[b]
2/4/A1	0.74	0.95[b]

[a] Data points were considered as significant outliers if more than 4 RMSEs away from the regression line. [b] Digoxin, glycylsarcosine, and methotrexate were removed from the correlation since they were significant outliers in 2/4/A1 rank order correlation between experimental P_{app} and FA.

Table 4. Percentage of Compounds that Were Correctly Classified Using in Silico Calculated P_{app} Data

		correctly classified as	
data set[a]	membrane model	acceptably absorbed[b]	poorly absorbed[e]
experimental data set	HDM	90%[c]	67%[f]
	Caco-2	100%[c]	67%[f]
	2/4/A1	95%[c]	89%[f]
external test set	HDM	89%[d]	14%[g]
	Caco-2	83%[d]	71%[g]
	2/4/A1	94%[d]	71%[g]

[a] Experimental data set, Table 1; external test set, Supporting Information. [b] Fraction of the compounds correctly classified as FA ≥ 30%. [c] $n = 20$. [d] $n = 18$. [e] Fraction of the compounds correctly classified as FA < 30%. [f] $n = 9$. [g] $n = 7$.

has not been fully determined yet for most of these substances, but based on previous experience we tentatively conclude that many active transporters may be saturated at therapeutic doses and would therefore not influence FA.[44] The permeabilities of the P-gp substrates in the data set were on average better correlated to FA when using Caco-2 P_{app} than when using 2/4/A1 P_{app}, which can be attributed to the fact that P-gp is functionally expressed in Caco-2 but not in 2/4/A1. However, the P-gp substrates metolazone and cimetidine were large outliers in the Caco-2 relationship, and the overall scatter was larger in the Caco-2 relationship than that for 2/4/A1. In the HDM relationship, a significant scatter was seen, for both actively and passively transported compounds.

In Silico Classification and Ranking. To further investigate the differences between the models, multivariate analysis was used to develop structure−permeability relationships. Similar to previously published models of cellular permeability, descriptors related to polarity and hydrogen bond interactions dominated the models based on Caco-2 and 2/4/A1 P_{app}.[22,26−31,35] Further, the cell-based models were dominated by permeability-limiting descriptors (i.e., descriptors having a negative value). In contrast, the PLS model of HDM P_{app} had a larger influence of permeability-driving descriptors, mainly describing nonpolar interactions between the drug and its environment. This difference between cell-based and artificial membrane models can be explained by the relative simplicity of the HDM experimental model, where the hexadecane models the rate-limiting diffusion step across the hydrophobic interior of the lipid bilayer.[62]

The in silico models based on Caco-2 and 2/4/A1 P_{app} classified the data set better as poorly or acceptably absorbed than the HDM-based model (Table 4), and the rank order correlation between FA and calculated P_{app} was stronger for the cell-based models than for the HDM-based in silico model. This was also true when the in silico models were challenged with an external test set. The best compound ranking results were obtained using the 2/4/A1-based in silico model, which gave a correlation coefficient close to that for the experimental P_{app} data ($r_s = 0.85$ and 0.74 when the in silico models were used to predict the experimental data set and the external test set, respectively, Figure 5).

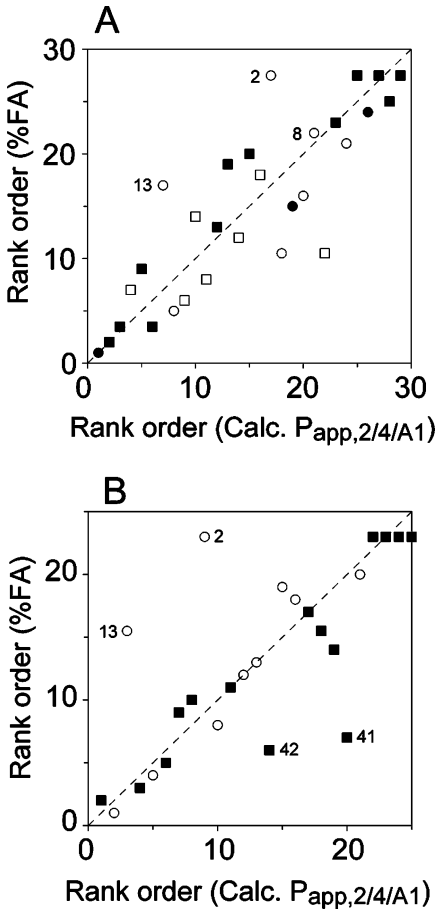

Figure 5. Spearman rank order correlation between FA and P_{app} calculated using the 2/4/A1-based in silico model. (A) Experimental data set (Table 1); (B) external test set (Supporting Information). Squares denote compounds in the training set and circles compounds in the test set. Closed symbols, passively transported compounds; open symbols, actively transported compounds.

Similar to the experimentally determined data set, several of the compounds in the external test set that were well described by the 2/4/A1 in silico model have been shown to be substrates for various active transporters, but the in vivo relevance of active transport for most of these substances in the human intestine has not been fully determined (Supporting Information). However, two compounds were overpredicted by the 2/4/A1 in silico model, pafenolol and enalaprilic acid (external test set, Table 8 in the Supporting Information), and two were underpredicted, glycylsarcosine and methotrexate (PLS test set, Table 1). As stated above, the underprediction of both glycylsarcosine and methotrexate can be explained by active uptake mechanisms that significantly influence permeability in vivo but which are not present in the 2/4/A1 cell model (Table 1). Pafenolol has been shown to be a substrate for the P-glycoprotein efflux transporter[44] and also to bind to

cholic acids in the intestinal lumen in vivo,[63] which could account for the overprediction of FA, whereas the overprediction of enalaprilic acid FA can, at least partly, be attributed to relatively large interpatient variability in the experimental FA determination (values of between 10 and 40% have been reported).[64] When these outliers were removed from the relationship, the correlation coefficient increased to an excellent 0.97.

Conclusions

Diametrically opposed views regarding the paracellular pathway are presented in the literature, ranging from complete disregard of the influence of paracellular drug permeability[65] to proposals that this pathway is a significant contributor to total drug permeability for many incompletely absorbed, low permeability compounds.[15,66,67] Our findings support the latter view and demonstrate a need to include the paracellular pathway in models used for drug permeability screening, especially in drug discovery programs where significant numbers of low-permeability compounds are expected. We propose that the small-intestine-like 2/4/A1 epithelial cell line, which has the largest influence of the paracellular pathway of the studied experimental models, is a suitable experimental model for studies of passive permeability in drug discovery. Further, because the 2/4/A1 model is at least 100-fold more permeable to low permeability drugs than Caco-2 and HDM, the demands for more sophisticated analytical equipment such as LC-MS-MS are probably eliminated. However, the results also show that none of the experimental models studied was able to predict FA for all of the compounds exhibiting significant active transport mechanisms in vivo. Separate assays for detecting active transporter affinities of discovery compounds are therefore warranted. Finally, the results from this study indicate that the in silico model based on 2/4/A1 P_{app} can be successfully used for both permeability classification and ranking and suggest that computational models obtained from this cell line are promising alternatives to simpler experimental models in early drug discovery.

Materials and Methods

Data Set Selection. The data set used for model building was selected to spread evenly over the range FA 0−100% (Figure 2h). The compounds were taken from the 11th revision of the World Health Organization's list of essential drugs[68] and from the list of compounds recommended by the FDA for permeability classification.[57] Compounds for which either in vitro or in vivo results indicated an influence from active transport mechanisms were also included in the data set, because such compounds may be present in compound selections in early drug discovery when transport characteristics are unknown. Other selection criteria were that the compounds should be structurally (Supporting Information) and physicochemically diverse (Figure 2i), that the compounds could be analyzed using molecular mechanics calculations, and that FA data of acceptable quality should be available in the literature. The diversity of the compounds used in this study was analyzed using the ChemGPS methodology[54] and molecular descriptors generated by the program SELMA (see the section "Conformational Analysis and Descriptor Generation" below). To verify that the data set was spread throughout the chemical space of orally administered drugs, a reference data set of 150 oral drugs from the Physician's Desk Reference[55] was included in the ChemGPS analysis.

[^{14}C]Creatinine, [^{3}H]digoxin, [^{14}C]mannitol, [^{3}H]propranolol, [^{3}H]sulfasalazine, and [^{3}H]raffinose, were purchased from New England Nuclear (Boston, MA). [^{14}C]Aciclovir, [^{14}C]foscarnet, [^{14}C]ganciclovir, [^{3}H]glycylsarcosine, [^{3}H]lobucavir, [^{3}H]methotrexate, [^{3}H]mitoxantrone, and [^{14}C]valaciclovir were purchased from Moravec Biochemicals (Brea, CA). [^{3}H]Lactulose was purchased from American Radiolabeled Chemicals Inc. (St. Louis, MO). [^{14}C]Clodronate (Leiras Co., Turku, Finland) was a gift from Dr. J. Mönkkönen (University of Kuopio, Finland). Didanosine, metformin, and nadolol were obtained from Bristol Myers Squibb (Princeton, NJ). Alprenolol, antipyrine, atenolol, metolazone, metoprolol, pindolol, sulpiride, and terbutaline were purchased from Sigma (St. Louis, MO). Olsalazine was a gift from Dr. W. Rolfsen (Pharmacia & Upjohn, Uppsala, Sweden).

Preparation of Filter-Immobilized Hexadecane Membranes (HDMs). HDMs were prepared essentially as described by Wohnsland and Faller, with a few modifications.[12,69] A 71.5-μL aliquot of 5% (v/v) hexadecane in hexane was added to polycarbonate filter inserts (Transwell Costar, Badhoevedorp, The Netherlands; pore density 1×10^8 pores/cm^2; mean pore diameter 0.4 μm;[69] theoretical porosity 16%; diameter 12 mm), resulting in a final volume of 3.575 μL of hexadecane/filter. The pore diameter stated by the manufacturer was confirmed for a number of filters using atomic force microscopy. A larger filter size than in the original paper was used to facilitate stirring in the wells. The impregnated inserts were left at room temperature in a fume hood for at least 1 h prior to the drug transport studies to ensure that the evaporation of hexane was complete. [^{14}C]Mannitol flux was used to measure the plate-to-plate variation of the HDMs, using three filters on each 12-filter plate. Transepithelial electrical resistance (TEER) was measured repeatedly during the adaptation of Wohnsland and Fallers HDM method to our laboratory setting.[53] The TEER values obtained were $\geq$5000 Ω for all of the filters prepared using the presented protocol (Figure 1).

Drug Transport Experiments. Drug transport experiments were performed as described previously.[21] Briefly, the drug was dissolved in Hank's balanced salt solution (HBSS) buffered to pH 7.4 using 25 mM HEPES. A buffer of pH 7.4 not containing the drug was added to the receiver side of the membrane or cells, and the drug solution (pH 7.4) was added to the donor side. The membranes were incubated in a humidified atmosphere at 37°C. At regular time intervals (10−120 min), samples were withdrawn from the receiver chamber, and the volume was replaced with fresh, preheated buffer of pH 7.4 without the drug. Pending analysis, samples were stored in a freezer (−20°C). The filter plates were stirred at high velocity (500 rpm) to minimize the influence of the aqueous boundary layer.[22] All of the experiments were performed in at least triplicate, and the integrity of the membranes was determined for each filter batch by measuring the membrane permeability to [^{14}C]mannitol. Mass balance was assessed by sampling the donor and receiver chamber after completing the transport experiment.

Drug transport experiments in Caco-2 and 2/4/A1 cell monolayers were performed using the same experimental setup as for the HDM experiments. Because the transport experiments were performed without a transmembrane pH gradient, uptake transporters utilizing the proton gradient (e.g., PepT1, RFC, and ENT2) were inactive in the Caco-2 model. However, unlike the 2/4/A1 and the HDM models, the Caco-2 monolayers express other functionally active efflux transporters such as P-glycoprotein, multidrug resistance associated proteins (MRPs), and breast cancer resistance protein (BCRP) under these conditions.

Analytical Methods. Radioactively labeled substances were analyzed using a liquid scintillation counter (Packard Instruments 1900CA TRICARB; Canberra Packard Instruments, Downers Grove, IL). For unlabeled substances, a reversed-phase HPLC system was used. The system consisted of two Bischoff HPLC compact pumps model 2250, a Bischoff DAD 3L-EU/3L-OU UV detector, a Bischoff LC-CaDI 22-14 integrator (Bischoff Analysentechnik und -Geräte GmbH,

Leonberg, Germany), a JASCO FP-1520 fluorescence detector (Jasco Corp., Tokyo, Japan), a Midas model 830 autosampler (Spark, Emmen, The Netherlands), and the McDAcq32 chromatography data system software, version 1.46 (Bischoff Analysentechnik und -Geräte GmbH, Leonberg, Germany). The analytical column used was a Reprosil 100 C8 column (50 mm × 3 mm; mean particle size 5 μm; Dr. A. Maisch, Ammerbuch, Germany). A mobile phase gradient composed of mobile phase A containing Milli-Q water/acetonitrile/TFA at ratios of 95:5:0.1 and B containing Milli-Q water/acetonitrile/TFA at ratios of 5:95:0.1 was used. During one gradient cycle of 4 min, the mobile phase was changed from 5% to 80% of mobile phase B over a period of 1.5 min, kept at 80% mobile phase B for 1 min, and thereafter lowered to 5% of B, where it was kept until the next sample was injected. A flow rate of 2.0 mL/min and injection volumes of 30 μL were used during the analysis. All of the concentration determinations were well within the detection range for the analysis method used.

Permeability Calculations. The apparent permeability coefficients (P_{app}, cm/s) for the HDM permeability experiments were calculated using the generally applicable nonsink condition analysis that imposes less restriction on the experimental conditions than the commonly used sink condition based calculation.[10,70] The advantage of the nonsink condition analysis is that it is applicable also when the experiment does not exhibit linear drug flux, e.g., for highly permeable compounds. P_{app} for the studied substances was determined by nonlinear curve fitting of eq 1 to the experimental data

$$C_R(t) = \frac{M}{V_D + V_R} + \left(C_{R,0} - \frac{M}{V_D + V_R}\right)e^{-P_{app}A(1/V_D + 1/V_R)t} \quad (1)$$

where V_D is the volume in the donor compartment (0.5 mL), V_R is the volume in the receiver compartment (1.5 mL), A is the area of the filter (1.13 cm^2), M is the total amount of drug in the system, $C_{R,0}$ is the drug concentration in the receiver compartment at the start of the time interval, and $C_R(t)$ is the drug concentration in the receiver compartment at time t measured from the start of the interval. The sampling procedure necessitates the recalculation of M and $C_{R,0}$ for each interval.

Mass balance was calculated as the amount of drug recovered in receiver samples after each interval and in the donor chamber at the end of the experiment divided by the amount of drug in the donor chamber at the beginning of the experiment.

Conformational Analysis and Descriptor Generation. A 500 step Monte Carlo conformational analysis was performed using the BatchMin program and the MMFF force field, as implemented in MacroModel.[71] The conformational searches were performed in vacuum with the molecules in their unionized state, and the global minimum energy conformer was used as input for the in-house software MAREA[72] to calculate the static free molecular surface areas of the different atom types, as described previously.[29]

The 2D descriptors were calculated using Molconn-Z [73] and the software package SELMA.[74] Molconn-Z calculates electrotopological state indices, i.e., values relating to the electronic and topological environments of the atoms in a molecule. The indices encode the electronegativity as well as the local topology of each atom by considering perturbation effects from neighboring atoms. SELMA generates various descriptors related to molecular size, ring structure, flexibility, atom and bond counts, polarity, hydrogen bonds, Kier connectivity indices, BCUT parameters related to connectivity and atom weights, electronic environment, charge, and lipophilicity. SELMA and Molconn-Z generated a total of 140 descriptors.

In Silico Permeability Models. In silico models of permeability were developed as described previously.[29] Partial least squares projection to latent structures (PLS), as implemented in Simca,[75] was used to derive multivariate structure−permeability relationships for the different experimental models. Separate PLS models were derived for HDM, Caco-2, and 2/4/A1 P_{app}. The data set was divided into a training set and a test set, and only the training set compounds were used for developing the PLS models. The test set compounds were used to validate the final PLS models using the root-mean-squared error of prediction (RMSE) as a measure of predictivity

$$\mathrm{RMSE} = \sqrt{\frac{1}{n}\sum_{i=1}^{n}(y_{i,\mathrm{predicted}} - y_{i,\mathrm{measured}})^2} \quad (2)$$

The predictivity of the in silico models were further validated using an external test set.

Data Analysis. Permeability coefficients are presented as mean ± standard deviation (n = 3−4).

Spearman's rank order correlation coefficients were calculated as the linear correlation coefficient for two separate rankings of n items, according to

$$r_s = \frac{\sum_{i=1}^{n}(R_i - \bar{R})(S_i - \bar{S})}{\sqrt{\sum_{i=1}^{n}(R_i - \bar{R})^2}\sqrt{\sum_{i=1}^{n}(S_i - \bar{S})^2}} \quad (3)$$

where R_i and S_i are the ranks associated with the x and y values for compound i, $\bar{R}$ and $\bar{S}$ are the mean ranks for the x and y values, respectively, and n is the number of compounds. A larger value of r_s indicates a greater association between the two rankings.

Generating Classification Models. An empirical sigmoidal function was used to describe the relationship between FA and the permeability data

$$\mathrm{FA} = \frac{100}{1 + \left(\frac{P_{app}}{P_{app,50\%}}\right)^{\gamma}} \quad (4)$$

where $P_{app,50\%}$ is the value of P_{app} at 50% FA and γ is a slope factor. The equation was fitted to the experimental data for the training set compounds by minimizing the sum of squared residuals ($\mathrm{FA}_{calculated} - \mathrm{FA}_{experimental}$), and the fit was assessed using R^2, the coefficient of determination. For HDM permeability data, an alternative function that better described the data was used:[76]

$$\mathrm{FA} = 100(1 - e^{-kP_{app}}) \quad (5)$$

The training set was divided into two classes according to FA: acceptably absorbed (FA above cutoff value) and poorly absorbed (FA below cutoff value). Two different FA cutoff values (80% and 30%) were used in this study. Optimal permeability limits for discrimination between compounds in the different classes were determined for each membrane model based on the sigmoidal relationships between FA and P_{app}. Separate sets of permeability limits were selected for experimental P_{app} and for P_{app} calculated from the PLS regressions. The fraction of the compounds correctly classified into each group was then assessed using experimental or calculated P_{app} from the different experimental and in silico models.

Acknowledgment. This work was supported by Grant No. 9478 from the Swedish Research Council, the Knut and Alice Wallenberg Foundation, and the Swedish Fund for Research without Animal Experiments. We gratefully acknowledge the skillful experimental assistance of Sara Lindberg and Gustav Ahlin.

Supporting Information Available: Structures of the data set compounds, physicochemical data for the data set compounds, a PCA score plot of the data set, graphs of the correlation between P_{app} determined in the different models,

a comparison of results obtained in this study with literature values, a graph of the effect of changing FA cutoff on classification efficacy, rank order correlation graphs for ClogP vs. FA, ClogP vs. HDM P_{app}, and PSA vs. FA, a table showing the influence of random error on the rank order correlations, a table of the PLS model statistics, a graph of influential molecular descriptors, a cross-correlation matrix for the molecular descriptors, and a table of data for the external test set. This information is available free of charge via the Internet at http://pubs.acs.org.

References

(1) Lipinski, C. A.; Lombardo, F.; Dominy, B. W.; Feeney, P. J. Experimental and Computational Approaches to Estimate Solubility and Permeability in Drug Discovery and Development Settings. *Adv. Drug Delivery Rev.* **1997**, *23*, 3−25.

(2) Artursson, P.; Borchardt, R. T. Intestinal Drug Absorption and Metabolism in Cell Cultures: Caco-2 and Beyond. *Pharm. Res.* **1997**, *14*, 1655−1658.

(3) Artursson, P.; Palm, K.; Luthman, K. Caco-2 Monolayers in Experimental and Theoretical Predictions of Drug Transport. *Adv. Drug Delivery Rev.* **2001**, *46*, 27−43.

(4) Pickett, S. D.; McLay, I. M.; Clark, D. E. Enhancing the Hit-to-Lead Properties of Lead Optimization Libraries. *J. Chem. Inf. Comput. Sci.* **2000**, *40*, 263−272.

(5) Ingels, F. M.; Augustijns, P. F. Biological, Pharmaceutical, and Analytical Considerations with Respect to the Transport Media Used in the Absorption Screening System, Caco-2. *J. Pharm. Sci.* **2003**, *92*, 1545−1558.

(6) van de Waterbeemd, H.; Smith, D. A.; Beaumont, K.; Walker, D. K. Property-Based Design: Optimization of Drug Absorption and Pharmacokinetics. *J. Med. Chem.* **2001**, *44*, 1313−1333.

(7) Engman, H. A.; Lennernäs, H.; Taipalensuu, J.; Otter, C.; Leidvik, B.; Artursson, P. CYP3A4, CYP3A5, and MDR1 in Human Small and Large Intestinal Cell Lines Suitable for Drug Transport Studies. *J. Pharm. Sci.* **2001**, *90*, 1736−1751.

(8) Schmiedlin-Ren, P.; Thummel, K. E.; Fisher, J. M.; Paine, M. F.; Lown, K. S.; Watkins, P. B. Expression of Enzymatically Active CYP3A4 by Caco-2 Cells Grown on Extracellular Matrix-Coated Permeable Supports in the Presence of 1α, 25-Dihydroxyvitamin D_3. *Mol. Pharmacol.* **1997**, *51*, 741−754.

(9) Grasset, E.; Pinto, M.; Dussaulx, E.; Zweibaum, A.; Desjeux, J. F. Epithelial Properties of Human Colonic Carcinoma Cell Line Caco-2: Electrical Parameters. *Am. J. Physiol.* **1984**, *247*, C260−C267.

(10) Tavelin, S.; Gråsjö, J.; Taipalensuu, J.; Ocklind, G.; Artursson, P. Applications of Epithelial Cell Culture in Studies of Drug Transport. *Methods Mol. Biol.* **2002**, *188*, 233−272.

(11) Tavelin, S.; Taipalensuu, J.; Hallböök, F.; Vellonen, K. S.; Moore, V.; Artursson, P. An Improved Cell Culture Model Based on 2/4/A1 Cell Monolayers for Studies of Intestinal Drug Transport: Characterization of Transport Routes. *Pharm. Res.* **2003**, *20*, 373−381.

(12) Wohnsland, F.; Faller, B. High-Throughput Permeability pH Profile and High-Throughput Alkane/Water log P with Artificial Membranes. *J. Med. Chem.* **2001**, *44*, 923−930.

(13) Nakanishi, T.; Doyle, L. A.; Hassel, B.; Wei, Y.; Bauer, K. S.; Wu, S.; Pumplin, D. W.; Fang, H. B.; Ross, D. D. Functional Characterization of Human Breast Cancer Resistance Protein (BCRP, ABCG2) Expressed in the Oocytes of Xenopus Laevis. *Mol. Pharmacol.* **2003**, *64*, 1452−1462.

(14) Polli, J. W.; Wring, S. A.; Humphreys, J. E.; Huang, L.; Morgan, J. B.; Webster, L. O.; Serabjit-Singh, C. S. Rational Use of In Vitro P-Glycoprotein Assays in Drug Discovery. *J. Pharmacol. Exp. Ther.* **2001**, *299*, 620−628.

(15) Tavelin, S.; Taipalensuu, J.; Söderberg, L.; Morrison, R.; Chong, S.; Artursson, P. Prediction of the Oral Absorption of Low-Permeability Drugs Using Small Intestine-Like 2/4/A1 Cell Monolayers. *Pharm. Res.* **2003**, *20*, 397−405.

(16) Sugano, K.; Hamada, H.; Machida, M.; Ushio, H.; Saitoh, K.; Terada, K. Optimized Conditions of Bio-Mimetic Artificial Membrane Permeation Assay. *Int. J. Pharm.* **2001**, *228*, 181−188.

(17) Ruell, J. A.; Tsinman, K. L.; Avdeef, A. PAMPA−A Drug Absorption In Vitro Model 5. Unstirred Water Layer in Iso-pH Mapping Assays and $pK_{a\ flux}$-Optimized Design (pOD-PAMPA). *Eur. J. Pharm. Sci.* **2003**, 20, 393−402.

(18) Kansy, M.; Senner, F.; Gubernator, K. Physicochemical High Throughput Screening: Parallel Artificial Membrane Permeation Assay in the Description of Passive Absorption Processes. *J. Med. Chem.* **1998**, *41*, 1007−1010.

(19) Camenisch, G.; Folkers, G.; van de Waterbeemd, H. Comparison of Passive Drug Transport Through Caco-2 Cells and Artificial Membranes. *Int. J. Pharm.* **1997**, *147*, 61−70.

(20) Avdeef, A. *Absorption and Drug Development*; Wiley/Interscience: Hoboken, NJ, 2003.

(21) Artursson, P.; Karlsson, J. Correlation between Oral Drug Absorption in Humans and Apparent Drug Permeability Coefficients in Human Intestinal Epithelial (Caco-2) Cells. *Biochem. Biophys. Res. Commun.* **1991**, *175*, 880−885.

(22) Stenberg, P.; Norinder, U.; Luthman, K.; Artursson, P. Experimental and Computational Screening Models for the Prediction of Intestinal Drug Absorption. *J. Med. Chem.* **2001**, *44*, 1927−1937.

(23) Yazdanian, M.; Glynn, S. L.; Wright, J. L.; Hawi, A. Correlating Partitioning and Caco-2 Cell Permeability of Structurally Diverse Small Molecular Weight Compounds. *Pharm. Res.* **1998**, *15*, 1490−1494.

(24) Goodwin, J. T.; Conradi, R. A.; Ho, N. F.; Burton, P. S. Physicochemical Determinants of Passive Membrane Permeability: Role of Solute Hydrogen-Bonding Potential and Volume. *J. Med. Chem.* **2001**, *44*, 3721−3729.

(25) Zhao, Y. H.; Le, J.; Abraham, M. H.; Hersey, A.; Eddershaw, P. J.; Luscombe, C. N.; Butina, D.; Beck, G.; Sherborne, B.; Cooper, I.; Platts, J. A.; Boutina, D. Evaluation of Human Intestinal Absorption Data and Subsequent Derivation of a Quantitative Structure−Activity Relationship (QSAR) with the Abraham Descriptors. *J. Pharm. Sci.* **2001**, *90*, 749−784.

(26) Palm, K.; Luthman, K.; Ungell, A. L.; Strandlund, G.; Artursson, P. Correlation of Drug Absorption with Molecular Surface Properties. *J. Pharm. Sci.* **1996**, *85*, 32−39.

(27) Palm, K.; Stenberg, P.; Luthman, K.; Artursson, P. Polar Molecular Surface Properties Predict the Intestinal Absorption of Drugs in Humans. *Pharm. Res.* **1997**, *14*, 568−571.

(28) Clark, D. E. Rapid Calculation of Polar Molecular Surface Area and Its Application to the Prediction of Transport Phenomena. 1. Prediction of Intestinal Absorption. *J. Pharm. Sci.* **1999**, *88*, 807−814.

(29) Bergström, C. A. S.; Strafford, M.; Lazorova, L.; Avdeef, A.; Luthman, K.; Artursson, P. Absorption Classification of Oral Drugs Based on Molecular Surface Properties. *J. Med. Chem.* **2003**, *46*, 558−570.

(30) Palm, K.; Luthman, K.; Ungell, A. L.; Strandlund, G.; Beigi, F.; Lundahl, P.; Artursson, P. Evaluation of Dynamic Polar Molecular Surface Area as Predictor of Drug Absorption: Comparison with Other Computational and Experimental Predictors. *J. Med. Chem.* **1998**, *41*, 5382−5392.

(31) Kelder, J.; Grootenhuis, P. D.; Bayada, D. M.; Delbressine, L. P.; Ploemen, J. P. Polar Molecular Surface as a Dominating Determinant for Oral Absorption and Brain Penetration of Drugs. *Pharm. Res.* **1999**, *16*, 1514−1519.

(32) Zhu, C.; Jiang, L.; Chen, T. M.; Hwang, K. K. A Comparative Study of Artificial Membrane Permeability Assay for High Throughput Profiling of Drug Absorption Potential. *Eur. J. Med. Chem.* **2002**, *37*, 399−407.

(33) Petri, N.; Tannergren, C.; Holst, B.; Mellon, F. A.; Bao, Y.; Plumb, G. W.; Bacon, J.; O'Leary, K. A.; Kroon, P. A.; Knutson, L.; Forsell, P.; Eriksson, T.; Lennernäs, H.; Williamson, G. Absorption/Metabolism of Sulforaphane and Quercetin, and Regulation of Phase II Enzymes, in Human Jejunum In Vivo. *Drug. Metab. Dispos.* **2003**, *31*, 805−813.

(34) Tannergren, C.; Petri, N.; Knutson, L.; Hedeland, M.; Bondesson, U.; Lennernäs, H. Multiple Transport Mechanisms Involved in the Intestinal Absorption and First-Pass Extraction of Fexofenadine. *Clin. Pharmacol. Ther.* **2003**, *74*, 423−436.

(35) Winiwarter, S.; Ax, F.; Lennernäs, H.; Hallberg, A.; Pettersson, C.; Karlén, A. Hydrogen Bonding Descriptors in the Prediction of Human In Vivo Intestinal Permeability. *J. Mol. Graph. Model.* **2003**, *21*, 273−287.

(36) Sun, D.; Lennernäs, H.; Welage, L. S.; Barnett, J. L.; Landowski, C. P.; Foster, D.; Fleisher, D.; Lee, K. D.; Amidon, G. L. Comparison of Human Duodenum and Caco-2 Gene Expression Profiles for 12,000 Gene Sequence Tags and Correlation with Permeability of 26 Drugs. *Pharm. Res.* **2002**, *19*, 1400−1416.

(37) Lennernäs, H.; Knutson, L.; Knutson, T.; Hussain, A.; Lesko, L.; Salmonson, T.; Amidon, G. L. The Effect of Amiloride on the In Vivo Effective Permeability of Amoxicillin in Human Jejunum: Experience from a Regional Perfusion Technique. *Eur. J. Pharm. Sci.* **2002**, *15*, 271−277.

(38) Takamatsu, N.; Kim, O. N.; Welage, L. S.; Idkaidek, N. M.; Hayashi, Y.; Barnett, J.; Yamamoto, R.; Lipka, E.; Lennernäs, H.; Hussain, A.; Lesko, L.; Amidon, G. L. Human Jejunal Permeability of Two Polar Drugs: Cimetidine and Ranitidine. *Pharm. Res.* **2001**, *18*, 742−744.

(39) Irvine, J. D.; Takahashi, L.; Lockhart, K.; Cheong, J.; Tolan, J. W.; Selick, H. E.; Grove, J. R. MDCK (Madin-Darby Canine Kidney) Cells: A Tool for Membrane Permeability Screening. *J. Pharm. Sci.* **1999**, *88*, 28−33.

(40) Wessel, M. D.; Jurs, P. C.; Tolan, J. W.; Muskal, S. M. Prediction of Human Intestinal Absorption of Drug Compounds from Molecular Structure. *J. Chem. Inf. Comput. Sci.* **1998**, *38*, 726−735.

(41) Taipalensuu, J.; Törnblom, H.; Lindberg, G.; Einarsson, C.; Sjöqvist, F.; Melhus, H.; Garberg, P.; Sjöström, B.; Lundgren, B.; Artursson, P. Correlation of Gene Expression of Ten Drug Efflux Proteins of the ATP−Binding Cassette Transporter Family in Normal Human Jejunum and in Human Intestinal Epithelial Caco-2 Cell Monolayers. *J. Pharmacol. Exp. Ther.* **2001**, *299*, 164−170.
(42) Petri, N.; Lennernäs, H. In Vivo Permeability Studies in the Gastrointestinal Tract of Humans. *Drug Bioavailability−Estimation of Solubility, Permeability, Absorption and Bioavailability*; Wiley-VCH: Weinheim, Germany, 2003; pp 155−188.
(43) Terada, T.; Sawada, K.; Saito, H.; Hashimoto, Y.; Inui, K. I. Functional Characteristics of Basolateral Peptide Transporter in the Human Intestinal Cell Line Caco-2. *Am. J. Physiol.* **1999**, *276*, G1435−G1441.
(44) Chiou, W. L.; Chung, S. M.; Wu, T. C.; Ma, C. A Comprehensive Account on the Role of Efflux Transporters in the Gastrointestinal Absorption of 13 Commonly Used Substrate Drugs in Humans. *Int. J. Clin. Pharmacol. Ther.* **2001**, *39*, 93−101.
(45) Collett, A.; Higgs, N. B.; Sims, E.; Rowland, M.; Warhurst, G. Modulation of the Permeability of H2 Receptor Antagonists Cimetidine and Ranitidine by P-Glycoprotein in Rat Intestine and the Human Colonic Cell Line Caco-2. *J. Pharmacol. Exp. Ther.* **1999**, *288*, 171−178.
(46) Ganapathy, M. E.; Huang, W.; Wang, H.; Ganapathy, V.; Leibach, F. H. Valacyclovir: A Substrate for the Intestinal and Renal Peptide Transporters PEPT1 and PEPT2. *Biochem. Biophys. Res. Commun.* **1998**, *246*, 470−475.
(47) Terao, T.; Hisanaga, E.; Sai, Y.; Tamai, I.; Tsuji, A. Active Secretion of Drugs from the Small Intestinal Epithelium in Rats by P-Glycoprotein Functioning as an Absorption Barrier. *J. Pharm. Pharmacol.* **1996**, *48*, 1083−1089.
(48) Mahony, W. B.; Domin, B. A.; McConnell, R. T.; Zimmerman, T. P. Acyclovir Transport into Human Erythrocytes. *J. Biol. Chem.* **1988**, *263*, 9285−9291.
(49) Mahony, W. B.; Domin, B. A.; Zimmerman, T. P. Ganciclovir Permeation of the Human Erythrocyte Membrane. *Biochem. Pharmacol.* **1991**, *41*, 263−271.
(50) Liang, E.; Proudfoot, J.; Yazdanian, M. Mechanisms of Transport and Structure-Permeability Relationship of Sulfasalazine and Its Analogs in Caco-2 Cell Monolayers. *Pharm. Res.* **2000**, *17*, 1168−1174.
(51) Swaan, P. W.; Tukker, J. J. Carrier-Mediated Transport Mechanism of Foscarnet (Trisodium Phosphonoformate Hexahydrate) in Rat Intestinal Tissue. *J. Pharmacol. Exp. Ther.* **1995**, *272*, 242−247.
(52) Tavelin, S.; Milovic, V.; Ocklind, G.; Olsson, S.; Artursson, P. A Conditionally Immortalized Epithelial Cell Line for Studies of Intestinal Drug Transport. *J. Pharmacol. Exp. Ther.* **1999**, *290*, 1212−1221.
(53) Nagahara, N.; Tavelin, S.; Artursson, P. The Contribution of the Paracellular Route to the pH-Dependent Epithelial Permeability to Cationic Drugs. *J. Pharm. Sci.* **2004**, *93*, 2972−2984.
(54) Oprea, T. I.; Gottfries, J. Chemography: The Art of Navigating in Chemical Space. *J. Comb. Chem.* **2001**, *3,* 157−166.
(55) *Physician's Desk Reference*; Thomson Healthcare: Montvale, NJ, 2003.
(56) Amidon, G. L.; Lennernäs, H.; Shah, V. P.; Crison, J. R. A Theoretical Basis for a Biopharmaceutic Drug Classification−the Correlation of In−Vitro Drug Product Dissolution and In−Vivo Bioavailability. *Pharm. Res.* **1995**, *12*, 413−420.
(57) FDA, Guidance for Industry. Waiver of in vivo bioavailability and bioequivalence studies for immediate-release solid oral dosage forms based on a biopharmaceutics classification system. http://www.fda.gov/cder/guidance/index.htm. Accessed March 14, 2004.
(58) Winiwarter, S.; Bonham, N. M.; Ax, F.; Hallberg, A.; Lennernäs, H.; Karlén, A. Correlation of Human Jejunal Permeability (In Vivo) of Drugs with Experimentally and Theoretically Derived Parameters. A Multivariate Data Analysis Approach. *J. Med. Chem.* **1998**, *41*, 4939−4949.
(59) Adson, A.; Raub, T. J.; Burton, P. S.; Barsuhn, C. L.; Hilgers, A. R.; Audus, K. L.; Ho, N. F. Quantitative Approaches to Delineate Paracellular Diffusion in Cultured Epithelial Cell Monolayers. *J. Pharm. Sci.* **1994**, *83*, 1529−1536.
(60) Sugano, K.; Takata, N.; Machida, M.; Saitoh, K.; Terada, K. Prediction of Passive Intestinal Absorption Using Bio-Mimetic Artificial Membrane Permeation Assay and the Paracellular Pathway Model. *Int. J. Pharm.* **2002**, *241*, 241−251.
(61) Goldman, I. D.; Matherly, L. H. The Cellular Pharmacology of Methotrexate. *Pharmacol. Ther.* **1985**, *28*, 77−102.
(62) Marrink, S. J.; Berendsen, H. J. C. Permeation Process of Small Molecules across Lipid Membranes Studied by Molecular Dynamics Simulations. *J. Phys. Chem.* **1996**, *100*, 16729−16738.
(63) Lennernäs, H.; Regårdh, C. G. Evidence for an Interaction between the Beta-Blocker Pafenolol and Bile Salts in the Intestinal Lumen of the Rat Leading to Dose-Dependent Oral Absorption and Double Peaks in the Plasma Concentration−Time Profile. *Pharm. Res.* **1993**, *10*, 879−883.
(64) Ranadive, S. A.; Chen, A. X.; Serajuddin, A. T. M. Relative Lipophilicities and Structural Pharmacological Considerations of Various Angiotensin-Converting Enzyme (ACE) Inhibitors. *Pharm. Res.* **1992**, *9*, 1480−1486.
(65) Lennernäs, H. Does Fluid Flow across the Intestinal Mucosa Affect Quantitative Oral Drug Absorption? Is It Time for a Reevaluation? *Pharm. Res.* **1995**, *12*, 1573−1582.
(66) He, Y. L.; Murby, S.; Warhurst, G.; Gifford, L.; Walker, D.; Ayrton, J.; Eastmond, R.; Rowland, M. Species Differences in Size Discrimination in the Paracellular Pathway Reflected by Oral Bioavailability of Poly(Ethylene Glycol) and D-Peptides. *J. Pharm. Sci.* **1998**, *87*, 626−633.
(67) Adson, A.; Burton, P. S.; Raub, T. J.; Barsuhn, C. L.; Audus, K. L.; Ho, N. F. Passive Diffusion of Weak Organic Electrolytes across Caco-2 Cell Monolayers: Uncoupling the Contributions of Hydrodynamic, Transcellular, and Paracellular Barriers. *J. Pharm. Sci.* **1995**, *84*, 1197−1204.
(68) WHO List of Essential Drugs, 11th ed.; http://www.who.int/medicines/organization/par/edl/infedl11alpha.html. Accessed March 14, 2004.
(69) In the original reference (ref 12 in the reference list), a larger filter pore size (3.0 μm) was used. In our hands, this pore size resulted in defects (large aqueous pores) in the hexadecane membrane and a high mannitol flux. We therefore used 0.4 μm filters instead, because with these filters we could maintain the integrity of the hexadecane membrane. The adaptation of Wohnsland and Fallers method to the conditions in our lab is described in detail in ref 53. A comparison of the results in this study with those of Wohnsland and Faller is available in the Supporting Information.
(70) A Microsoft Excel macro for calculating P_{app} using eq 1, together with instructions for use, can be provided by us, free of charge. Contact Johan Gråsjö (e-mail: johan.grasjo@farmaci.uu.se).
(71) *Macromodel*, version 6.5; Schrödinger Inc., Portland, OR.
(72) The program MAREA is available upon request from the authors. The program is provided free of charge for academic users. Contact Johan Gråsjö (e-mail: johan.grasjo@farmaci.uu.se).
(73) *Molconn-Z*, version 3.15s; Hall Associates Consulting, Quincy, MA.
(74) Olsson, T.; Sherbukhin, V. Synthesis and Structure Administration (SaSA), AstraZeneca R&D: Mölndal, Sweden.
(75) *Simca-P*, version 10; Umetrics AB, Box 7960, SE−907 19 Umeå, Sweden.
(76) The HDM P_{app} limits for completely absorbed (FA > 80%) and poorly absorbed (FA < 30%) compounds obtained from eq 4 could not be used for permeability classification, because the limits were outside the range of HDM P_{app} values obtained in this study. In order not to disqualify the HDM model unfairly, the alternative eq 5 was used, which by visual inspection resulted in a better fit to the experimental HDM data.

JM049711O